The Astronomical Journal, 149:83 (6pp), 2015 February doi:10.1088/0004-6256/149/2/83

HD 207651: A COMPOSITE SPECTRUM TRIPLE SYSTEM

FRANCIS C. FEKEL[1]
Center of Excellence in Information Systems, Tennessee State University, 3500 John A. Merritt Boulevard, Box 9501, Nashville, TN 37209, USA; fekel@evans.tsuniv.edu
Received 2014 November 25; accepted 2015 January 6; published 2015 January 30

ABSTRACT

From numerous radial velocities obtained at KPNO and Fairborn Observatory, we have determined the orbital elements of the composite spectrum triple system HD 207651. This system consists of a broad-lined A8 V star and an unseen M dwarf companion in a 1.470739 days orbit. Variations of the center-of-mass velocity of this short-period system and velocity variations of a narrow-lined F7: V star have an orbital period of 724.1 days or 1.98 yr and an eccentricity of 0.39. The revised *Hipparcos* parallax, corresponding to a distance of 255 pc, appears to be too small to yield consistent properties. Instead, we adopt a distance of 150 pc.

Key words: binaries: spectroscopic – stars: early-type – stars: fundamental parameters – stars: individual (HD 207651) – stars: late-type

1. INTRODUCTION

HD 207651 = HIP 107786 = NSV 25772 ($\alpha = 21^h50^m08\overset{s}{.}23$, $\delta = 19°25'26\overset{''}{.}4$ (2000)) rose from obscurity to an object of some interest when Handler (1999) analyzed its *Hipparcos* photometry (Perryman & ESA 1997) and discovered it to have light variations with a period of 0.735 days. Because of that period he listed it as a possible γ Doradus pulsator, but he also mentioned that it might be a δ Scuti variable. Handler & Shobbrook (2002) included HD 207651 in their ground-based photometric search for stars with both short-period δ Scuti pulsations and longer-period γ Doradus variability. They found it to have short-term δ Scuti-type variability with a timescale of 1.5–2 hr as well as additional longer-term variability. However, the extent of their data was insufficient to determine the specific cause of the long-term variability. Handler & Shobbrook (2002) also compared the absolute magnitude of HD 207651 with its Strömgren photometry and suggested that the star might be a binary.

As part of a spectroscopic survey of more than 30 γ Doradus candidates identified by Handler (1999), Fekel et al. (2003) obtained a single spectrum of HD 207651. Along with several other stars in their survey, HD 207651 was found to be composite with its spectrum consisting of a narrow component situated near the center of each broad-lined component. The follow-up photometric and spectroscopic observations of Henry et al. (2004) confirmed the δ Sct variability and identified the longer-term light variations as the result of the ellipticity effect. Despite this clear variability, the star has not yet been assigned a variable star name.

Henry et al. (2004) increased the number of spectroscopic observations to nine. Radial velocities of the two components indicated that the system is triple with the broad-lined star having a period of 1.47 days, twice that of the ellipticity effect, while the velocities of the narrow-lined star suggested a period between 400 and 1500 days.

Fekel et al. (2003) estimated an A9 spectral class for the broad-lined star and noted that the *Hipparcos* parallax indicates that it is a giant. Henry et al. (2004) determined a slightly earlier spectral class of A8, while they classified the narrow-lined component as F7:, the colon indicating greater than usual uncertainty. Fekel et al. (2003) measured $v \sin i$ values of 95 and 6 km s^{-1} for the A star and the F star, respectively.

The broad-lined and pulsating nature of the short-period system make velocity measurements difficult. Nevertheless, we have obtained additional spectroscopic observations to determine the orbital elements of this triple system.

2. SPECTROSCOPIC OBSERVATIONS AND REDUCTIONS

We began our observation of HD 207651 at the KPNO in 2000 July and continued through 2012 May. At KPNO we used the coudé feed telescope, coudé spectrograph, and several different detectors to acquire 51 spectrograms. We obtained the vast majority with a Texas Instruments (TI) CCD. Those spectra are centered primarily in the red at 6430 Å, cover a wavelength range of just 84 Å, and have a resolution of 0.21 Å or a resolving power of about 30,000. Two of the spectrograms are centered at a blue wavelength of 4500 Å and have the same wavelength range and resolution, producing a resolving power of 21,000. In 2008 September the TI CCD was unavailable, and so we acquired a single spectrum of HD 207651 with a Tektronics CCD, identified as T1KA. That spectrum was centered at 6400 Å with the wavelength coverage increased to 172 Å, but the resolving power decreased to 19,000. After the TI CCD was retired in 2010 September, we obtained spectra with a CCD made by Semiconductor Technology Associates, designated STA2, which consists of a 2600 × 4000 array of 12 μm pixels. The increased array size produced a wavelength range of 336 Å for spectra centered at 6430 Å. The resolution was the same as our red wavelength TI CCD spectra, but there is some worsening of the resolution at both ends of these recent STA2 spectra. The spectra have typical signal-to-noise ratios (S/N) of about 150.

From 2009 October through 2014 October, we acquired 83 useful observations of HD 207651 with the Tennessee State University 2 m telescope, fiber-fed echelle spectrograph, and a CCD detector at Fairborn Observatory in southeastern Arizona (Eaton & Williamson 2004, 2007). Initially, the detector was a 2048 × 4096 SITe ST-002A CCD with 15 μm pixels.

[1] Visiting Astronomer, KPNO, NOAO, operated by the Association of Universities for Research in Astronomy, Inc. under cooperative agreement with the National Science Foundation.

Reduction of the raw spectra and wavelength calibration have been discussed by Eaton & Williamson (2007). The echelle spectrograms have 21 orders that cover the wavelength range 4920–7100 Å with an average resolution of 0.17 Å, corresponding to a resolving power of 35,000 at 6000 Å. While a typical S/N value for these spectra is 60, large temperature variations of the dewar caused reduced S/N of some spectra.

During the summer of 2011, the SITe CCD and its dewar were replaced with a Fairchild 486 CCD that has a 4096 × 4096 array of 15 μm pixels and a new dewar (Fekel et al. 2013). The expanded wavelength coverage enabled by the new CCD ranges from 3800 to 8600 Å, and the resolution of these echelle spectra is 0.24 Å or a resolving power of 25,000 at 6000 Å. This new combination produced improved S/N generally ranging from 100 to 150.

As shown by Fekel et al. (2003) and Henry et al. (2004), the spectrum of HD 207651 is double lined, consisting of a broad-lined component and a narrow-lined component. We measured the KPNO velocities with the IRAF[2] cross-correlation program FXCOR (Fitzpatrick 1993) by fitting separate Gaussians to between 1 and 4 lines of the two stars. While this was straightforward for the narrow-lined component, measurement of the broad-lined component was more problematic. In addition to its rapid rotation, the latter star is also a δ Scuti pulsator. Although our exposure times cover a significant fraction, between 20% and 50%, of the 1.55 hr pulsation cycle (Henry et al. 2004), the line profiles vary from observation to observation, and some are rather asymmetric. As a result, we used weights for the Gaussian fits that deemphasized the line center and instead fitted primarily the wings of the broad lines. Our KPNO velocities are listed in Table 1.

For our red-wavelength observations we used the IAU radial-velocity standards ι Piscium and HR 7560 as the cross-correlation reference stars, which according to Scarfe (2010) have radial velocities of 5.6 and 0.0 km s^{-1}, respectively. For our blue wavelength spectra the reference star was 68 Tau, which has a velocity of 39.0 km s^{-1} (Fekel 1999).

Unlike the KPNO velocities those from Fairborn Observatory are on an absolute scale. We used a solar-type star line list, consisting of 168 lines, for both components. We simultaneously fitted the line pairs of the components with rotational broadening functions (Fekel & Griffin 2011; Lacy & Fekel 2011) and allowed both the line width and depth to be free parameters. Our Fairborn velocities are given in Table 1.

From our unpublished measurements of the radial velocities of several IAU solar-type velocity standards compared with the results of Scarfe (2010), we add +0.3 km s^{-1} to our SITe CCD velocities and +0.6 km s^{-1} to our Fairchild CCD velocities, to adjust the velocity zero points so that the KPNO and Fairborn results are on a consistent scale.

3. SPECTROSCOPIC ORBIT

We initially obtained separate long-period orbital solutions of the KPNO and Fairborn radial velocities of the narrow-lined star, component B, with the computer program BISP (Wolfe et al. 1967), which uses the Wilsing–Russell method (Wilsing 1893; Russell 1902). Those two solutions were then refined with the program SB1 (Barker et al. 1967). The center-of-mass velocities of the two solutions differed by just 0.3 km s^{-1}, and the variances for the two solutions were very similar. Thus, the radial velocities from both observatories were given unit weights and a combined solution was obtained. The resulting orbital elements and related quantities are presented in Table 2. The radial velocities of B are listed in Table 1 along with their residuals to the orbit and are compared with the computed velocity curve in Figure 1.

We then employed the general least squares program of Daniels (1966) to obtain a simultaneous orbital solution of the primary's short- and long-period velocity variations. Velocities of this broad-lined star, component Aa, which is the brighter star of both the short-period and long-period systems, are much less precise because of that star's very large projected rotational velocity and its δ Sct pulsations, which significantly affect the shape of the line profiles. Thus, the values for four long-period orbital elements of component B, the period P, time of periastron T, eccentricity e, and longitude of periastron ω (plus 180°), were adopted in the solutions of component Aa.

As was done for component B, solutions were obtained separately for the KPNO and Fairborn velocities of component Aa. While some of the orbital elements of the two solutions, such as the center-of-mass velocity of the system and the period of the short-period orbit, differ by just 1 σ, other elements, such as the short-period eccentricity and short-period semiamplitude, differ by 2–3σ.

With a rather short period of 1.47 days, the close pair would be expected to have a circular orbit if it were just a binary system (Matthews & Mathieu 1992). But the effects of the long-period companion in the HD 207651 system could produce a modulation of the eccentricity (e.g., Mazeh & Shaham 1979). The short-period eccentricity determined from the Fairborn velocities, which we believe to be the more precise result, is 0.023 ± 0.022. Given the small value of this eccentricity and its nearly identical uncertainty, following the precepts of Lucy & Sweeney (1971), we have chosen to adopt a circular short-period orbit.

For component Aa the variances of the KPNO and Fairborn solutions are similar, suggesting that the individual velocities should be given nearly equal weights in a combined solution. However, the radial velocities, which normally characterize just the orbital motion of a binary component, also include a contribution, possibly very significant, from pulsation (e.g., Mathias et al. 2004), and so the variances reflect that combination. Because the KPNO velocities of Aa are determined from just 3 or 4 lines versus 168 lines for the Fairborn velocities, we examined orbital solutions that used three different sets of weights. In all three solutions we adopted weights of 1.0 for the Fairborn velocities, while the weights assigned to all KPNO velocities were either 1.0, or 0.5, or 0.2. Examining the results of those three solutions, we have chosen to adopt weights of 1.0 and 0.5 for the Fairborn and KPNO velocities, respectively, because the uncertainties of the parameters for that solution encompass the results of the other two solutions. The orbital elements and related quantities from the adopted solution are listed in Table 2. The individual velocities of Aa and their residuals to the combined fit of the short- and long-period velocity variations are given in Table 1. The radial velocities are compared with the long- and short-period velocity curves in Figures 1 and 2, respectively.

4. DISCUSSION

The *Hipparcos* parallax of HD 207651 was revised by van Leeuwen (2007), who determined a value of 0.″00392 ±

[2] IRAF is distributed by the NOAOs.

Table 1
Radial Velocities of HD 207651

Hel. Julian Date (HJD −2400000)	Phase$_L$	V_B (km s^{-1})	$(O-C)_B$ (km s^{-1})	V_{Aa} (km s^{-1})	$(O-C)_{Aa}$ (km s^{-1})	Phase$_S$	Observatory
51737.902	0.325	−20.7	−0.6	−24.4	1.15	0.513	KPNO
52539.770	0.432	−22.7	0.1	−11.2	−3.63	0.727	KPNO
52540.756	0.434	−23.1	−0.3	−16.8	3.44	0.397	KPNO
52541.706	0.435	−23.4	−0.6	13.5	−0.31	0.043	KPNO
52541.786[a]	0.435	−23.1	-0.3	10.5	−0.49	0.098	KPNO
52542.705	0.436	−24.2	−1.4	−8.8	−0.73	0.723	KPNO
52904.765	0.936	6.3	−0.2	−0.1	5.63	0.898	KPNO
52941.668	0.987	12.1	−1.6	−5.4	0.57	0.990	KPNO
52942.690	0.989	12.9	−0.8	−32.7	0.30	0.685	KPNO
53168.946	0.301	−19.2	−0.1	−28.7	−2.74	0.523	KPNO
53170.933	0.304	−18.9	0.4	5.7	−1.10	0.874	KPNO
53272.752	0.445	−23.5	−0.6	9.0	−1.62	0.104	KPNO
53276.726	0.450	−23.4	−0.4	0.0	−1.96	0.806	KPNO
53490.992	0.746	−16.9	0.6	−24.7	2.38	0.492	KPNO
53492.989	0.749	−17.1	0.2	4.7	1.26	0.850	KPNO
53531.946	0.803	−13.2	0.0	−17.5	2.80	0.338	KPNO
53534.958	0.807	−13.2	−0.4	−23.6	1.34	0.386	KPNO
53634.801	0.945	8.1	0.1	−22.1	2.64	0.272	KPNO
53636.767	0.947	8.9	0.4	−37.1	0.22	0.609	KPNO
53854.997	0.249	−16.5	−0.2	9.3	−1.51	0.990	KPNO
53855.989	0.250	−15.9	0.4	−19.8	−1.50	0.665	KPNO
54002.779	0.453	−23.9	−0.9	−27.2	−3.53	0.472	KPNO
54004.729	0.456	−23.5	−0.4	0.2	−0.81	0.797	KPNO
54005.774[a]	0.457	−24.6	-1.5	−24.2	−0.27	0.508	KPNO
54006.815	0.458	−23.5	−0.4	−3.0	−2.49	0.216	KPNO
54223.995	0.758	−17.0	−0.3	3.0	−3.09	0.883	KPNO
54265.952	0.816	−12.4	−0.5	−21.0	6.28	0.411	KPNO
54266.944	0.818	−11.4	0.3	3.4	−2.20	0.085	KPNO
54269.952	0.822	−11.6	−0.3	−1.8	−3.72	0.131	KPNO
54364.691	0.953	8.0	−1.4	−39.2	2.15	0.547	KPNO
54369.805	0.960	10.3	−0.2	−9.1	−4.71	0.024	KPNO
54407.630	0.012	13.1	−0.8	−21.5	4.85	0.742	KPNO
54408.648	0.013	13.0	−0.8	−36.9	6.13	0.434	KPNO
54583.991	0.256	−16.4	0.3	−18.7	0.35	0.655	KPNO
54643.928	0.338	−21.2	−0.6	−27.1	−4.88	0.408	KPNO
54732.778	0.461	−22.6	0.5	3.3	−0.30	0.820	KPNO
54734.731	0.464	−22.9	0.2	5.4	−1.53	0.148	KPNO
54949.993	0.761	−16.7	−0.2	−26.9	0.69	0.511	KPNO
55003.897	0.835	−9.7	0.1	−4.4	−2.42	0.162	KPNO
55006.932	0.840	−9.1	0.2	−13.7	−4.25	0.226	KPNO
55093.824	0.960	11.2	0.7	−24.4	5.77	0.306	KPNO
55094.773	0.961	11.0	0.3	−1.8	3.37	0.952	KPNO
55127.585	0.006	15.2	1.1	−24.0	2.87	0.261	Fair
55130.670	0.011	13.2	−0.8	−41.9	−4.27	0.359	Fair
55138.619	0.021	13.3	0.0	−18.9	4.48	0.764	Fair
55141.674	0.026	12.2	−0.7	−10.1	4.29	0.841	Fair
55161.635	0.053	8.3	−0.9	−37.7	1.53	0.413	Fair
55301.947	0.247	−15.9	0.2	−0.6	0.21	0.815	Fair
55311.994	0.261	−16.9	0.1	−20.2	−0.49	0.647	KPNO
55314.954	0.265	−17.8	−0.5	−14.3	4.02	0.659	Fair
55321.912	0.275	−17.9	−0.1	−19.3	3.19	0.390	Fair
55330.867	0.287	−19.7	−1.2	−25.0	1.37	0.479	Fair
55336.914	0.295	−18.0	0.9	−24.3	−1.03	0.591	Fair
55357.807	0.324	−19.8	0.3	−3.7	−2.93	0.796	Fair
55364.961	0.334	−20.7	−0.2	−14.2	2.20	0.661	Fair
55366.964	0.337	−20.0	0.6	10.6	−2.46	0.022	KPNO
55373.966	0.347	−21.3	−0.4	−2.2	−0.34	0.783	Fair
55382.949	0.359	−20.3	1.0	10.9	1.60	0.891	Fair
55412.958	0.400	−22.0	0.2	−5.9	4.61	0.295	Fair
55458.740	0.464	−22.1	1.0	−24.0	−2.25	0.424	Fair
55464.783	0.472	−23.4	−0.2	−23.9	−0.41	0.533	KPNO
55468.889	0.478	−22.8	0.4	−12.0	1.26	0.324	Fair
55477.686	0.490	−23.0	0.3	−11.9	−0.74	0.306	Fair

Table 1
(Continued)

55480.785	0.494	−22.8	0.5	−18.4	2.61	0.413	Fair
55489.704	0.506	−23.8	−0.5	−19.3	4.32	0.477	Fair
55500.717	0.522	−22.8	0.5	15.1	0.77	0.965	Fair
55513.735	0.540	−22.8	0.4	5.4	2.11	0.817	Fair
55526.723	0.557	−23.1	0.0	−16.3	−0.08	0.647	Fair
55554.650	0.596	−22.5	0.2	−17.1	0.46	0.636	Fair
55653.982	0.733	−17.9	0.3	0.0	−1.41	0.175	Fair
55663.978	0.747	−16.0	1.4	17.1	5.93	0.971	Fair
55666.974	0.751	−16.7	0.4	10.7	−0.61	0.008	Fair
55679.925	0.769	−15.7	0.2	−2.3	−1.23	0.814	Fair
55679.995	0.769	−15.9	0.0	3.0	−0.83	0.862	KPNO
55680.993	0.771	−16.6	−0.8	−34.0	−6.60	0.540	KPNO
55686.936	0.779	−15.3	−0.1	−25.7	0.20	0.581	Fair
55689.917	0.783	−14.8	0.1	−23.0	1.26	0.608	Fair
55693.881	0.788	−14.7	−0.2	−15.5	0.33	0.303	Fair
55695.916	0.791	−14.0	0.2	−18.3	−1.24	0.687	Fair
55710.872	0.812	−12.1	0.2	0.2	−1.06	0.856	Fair
55718.922	0.823	−11.7	−0.5	−18.3	2.26	0.329	Fair
55724.854	0.831	−10.6	−0.3	−24.7	−0.31	0.363	Fair
55731.965	0.841	−8.8	0.3	−6.7	−0.45	0.198	KPNO
55732.950	0.842	−8.4	0.5	2.8	2.37	0.868	KPNO
55734.946	0.845	−9.4	−0.8	−9.5	0.20	0.225	KPNO
55755.822	0.874	−4.9	−0.3	−34.2	−2.32	0.419	Fair
55833.829	0.982	14.5	1.3	−47.3	−3.65	0.458	Fair
55844.650	0.997	14.7	0.4	−16.2	1.52	0.816	Fair
55845.605	0.998	14.0	−0.1	−49.0	−4.67	0.465	Fair
55846.604	0.999	14.3	0.2	−13.0	0.60	0.144	Fair
55847.593	0.001	14.6	0.5	−21.8	−4.16	0.817	Fair
55848.592	0.002	14.4	0.3	−46.0	−1.19	0.496	Fair
55849.591	0.003	14.6	0.5	−21.1	−4.33	0.175	Fair
55851.590	0.006	14.4	0.3	−45.7	−1.35	0.534	Fair
55852.592	0.008	14.2	0.1	−19.3	2.05	0.216	Fair
55853.588	0.009	13.8	−0.2	−8.1	2.24	0.893	Fair
55854.588	0.010	14.5	0.5	−39.9	2.84	0.573	Fair
55855.587	0.012	14.4	0.5	−29.7	−4.05	0.252	Fair
55856.770	0.013	14.5	0.6	−3.7	3.54	0.056	Fair
55857.586	0.014	14.5	0.7	−42.2	−2.11	0.611	Fair
55858.603	0.016	13.6	−0.1	−30.3	1.26	0.303	Fair
55868.761	0.030	12.1	−0.4	−20.7	−0.96	0.210	Fair
55881.764	0.048	9.5	−0.6	−1.0	3.88	0.051	Fair
55933.607	0.119	−2.6	−0.2	−20.8	1.46	0.300	Fair
56012.004	0.228	−15.4	−0.6	−23.0	1.58	0.605	Fair
56012.997	0.229	−14.6	0.3	−11.9	0.97	0.280	Fair
56053.926	0.286	−18.5	−0.1	6.8	−0.90	0.109	Fair
56060.970	0.295	−19.0	−0.1	3.7	−4.80	0.898	KPNO
56082.823	0.325	−20.7	−0.6	−5.6	−0.14	0.757	Fair
56204.786	0.494	−22.5	0.8	−10.2	2.20	0.683	Fair
56251.704	0.559	−22.6	0.5	−18.8	2.50	0.584	Fair
56274.692	0.590	−22.8	−0.1	−0.9	−0.35	0.214	Fair
56385.982	0.744	−17.7	−0.1	5.7	−0.96	0.884	Fair
56415.931	0.786	−14.5	0.2	−11.0	−2.00	0.247	Fair
56446.968	0.828	−9.7	0.9	−19.5	3.51	0.350	Fair
56469.766	0.860	−7.3	−0.7	−6.3	−3.89	0.851	Fair
56551.868	0.973	12.5	0.1	−35.0	−1.69	0.675	Fair
56576.809	0.008	14.3	0.2	−42.9	−4.48	0.633	Fair
56604.702	0.046	10.1	−0.2	−44.7	−5.59	0.598	Fair
56633.619	0.086	2.7	−0.6	−17.5	3.14	0.260	Fair
56634.620	0.088	2.7	−0.4	−0.5	0.84	0.940	Fair
56635.605	0.089	3.7	0.9	−34.1	−0.06	0.610	Fair
56656.607	0.118	−1.6	0.5	−0.1	1.41	0.890	Fair
56668.590	0.134	−3.4	1.3	2.9	−0.90	0.038	Fair
56743.999	0.239	−14.8	0.8	−19.4	−3.38	0.311	Fair
56745.991	0.241	−15.5	0.2	−19.4	−0.82	0.665	Fair
56747.986	0.244	−15.5	0.4	8.9	−1.60	0.021	Fair
56752.971	0.251	−16.7	−0.3	−25.6	−0.86	0.411	Fair
56753.969	0.252	−16.6	−0.1	4.5	−3.51	0.089	Fair

Table 1
(Continued)

56754.972	0.254	−16.5	0.1	−9.6	−3.91	0.771	Fair
56783.906	0.294	−17.9	0.9	−26.9	−1.71	0.445	Fair
56812.823	0.334	−20.8	−0.4	5.9	−3.16	0.106	Fair
56900.779	0.455	−22.6	0.4	16.4	4.75	0.910	Fair
56940.786	0.510	−23.4	−0.1	9.8	−0.4	0.510	Fair

[a] 4500 Å region.

Table 2
HD 207651 Orbital Elements and Related Parameters

Parameter	Component Aa	Component B
P_L (days)	724.09 (fixed)	724.09 ± 0.33
T_L (HJD)	2454398.97 (fixed)	2454398.97 ± 1.13
e_L	0.3866 (fixed)	0.3866 ± 0.0041
ω_L (deg)	178.25 (fixed)	358.25 ± 0.65
K_L (km s^{-1})	10.50 ± 0.32	18.715 ± 0.072
γ (km s^{-1})	−10.95 ± 0.25	−11.819 ± 0.055
$a_L \sin i$ (10^6 km)	96.40 ± 3.91	171.86 ± 0.74
$f(m)_L$ ($M_\odot$)	0.0681 ± 0.0082	0.3858 ± 0.0050
$m_L \sin^3 i$ ($M_\odot$)	0.940[b] ± 0.020	0.527 ± 0.024
P_S (days)	1.4707386 ± 0.0000064	…
T_0[a] (HJD)	2,452,553.441 ± 0.014	…
e_S	0.0 adopted	…
ω_S (deg)	0.0 adopted	…
K_S (km s^{-1})	19.31 ± 0.36	…
$a_S \sin i$ (10^6 km)	0.3906 ± 0.0079	…
$f(m)_S$ ($M_\odot$)	0.001097 ± 0.000066	…
Standard error of an observation of unit weight (km s^{-1})	2.4	0.6

[a] Time of maximum velocity.
[b] Combined mass of components Aa and Ab.

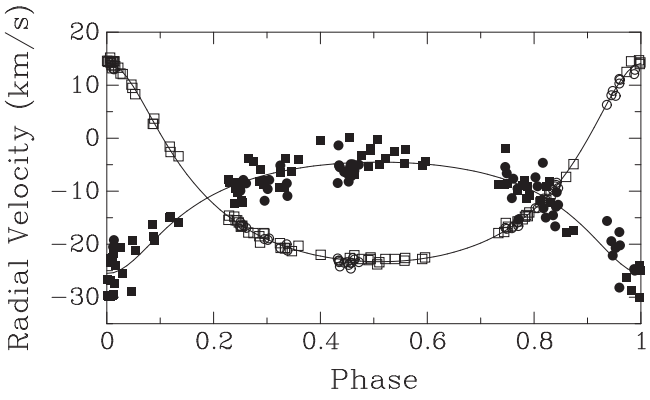

Figure 1. Long-period orbit of HD 207651. Solid symbols are velocities of component Aa. Those points represent the observed velocities minus the velocities in the short-period orbit that were calculated from the elements in Table 2. Open symbols are velocities of B. Dots—KPNO, squares—Fairborn Observatory. Solid lines are the calculated velocity curves. Zero phase is a time of periastron passage.

0.″00066. The combined system has $V = 7.21$ mag and $B - V = 0.236$ mag (Perryman & ESA 1997). Given the rather different spectral classes of the components, A8 and F7:, we increase the magnitude difference of 2.0 mag (Henry et al. 2004), which was a minimum value, to 2.3 mag to account for the greater line strength of the component with the later spectral type. Assuming no interstellar extinction, as indicated by the agreement of the primary's spectral class of A8 (Henry et al. 2004) with the combined $B - V$, results in $m_V = 7.33 \pm 0.05$ mag, where the uncertainty accounts for the uncertain magnitude difference. With the revised *Hipparcos* parallax we then determine that the broad-lined primary component Aa, has $M_V = 0.3 \pm 0.4$ mag. For component B our adopted magnitude difference results in $m_V = 9.63$ mag with an estimated uncertainty of 0.4 mag and produces $M_V = 2.6 \pm 0.5$ mag.

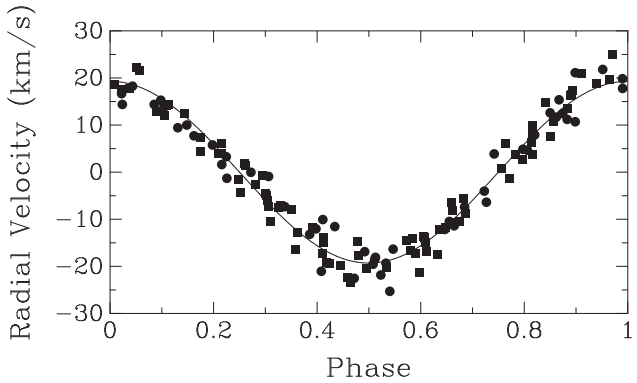

Figure 2. Radial-velocity curve of HD 207651 Aa in the short-period orbit. The points represent the observed velocities minus the velocities of the center-of-mass in the long period orbit, calculated from the elements in Table 2. Solid dots—KPNO, solid squares—Fairborn Observatory. The solid line is the calculated velocity curve. The period is 1.4707386 days and zero phase is a time of maximum velocity.

Our Fairborn Observatory spectra show that the composite Hα line has broad wings indicating that the much brighter star, component Aa, is a dwarf, and therefore so is the fainter, less massive component B. Comparison of our computed M_V values, determined from the revised parallax, with canonical results for A8 V and F7 V stars (e.g., Gray 1992) indicates that the stars are 1.3–2 mag too bright.

A second comparison can be made by adopting $B - V = 0.50$ mag from the spectral type of the F7 V star. With the use of the relations from Flower (1996) we then convert the colors of components Aa and B to their corresponding temperatures and also compute for the two stars their luminosities from the M_V values and bolometric corrections. We then compare the positions of Aa and B in an H-R diagram (Figure 3) with the solar-abundance evolutionary tracks of Girardi et al. (2000). That comparison suggests masses of 2.4 and 1.5 $M_\odot$, which are significantly too large for the spectral classes (Gray 1992).

Both of the above comparisons argue that the actual distance to the system is significantly less than the 255 pc indicated by the revised *Hipparcos* result. Note that the original *Hipparcos*

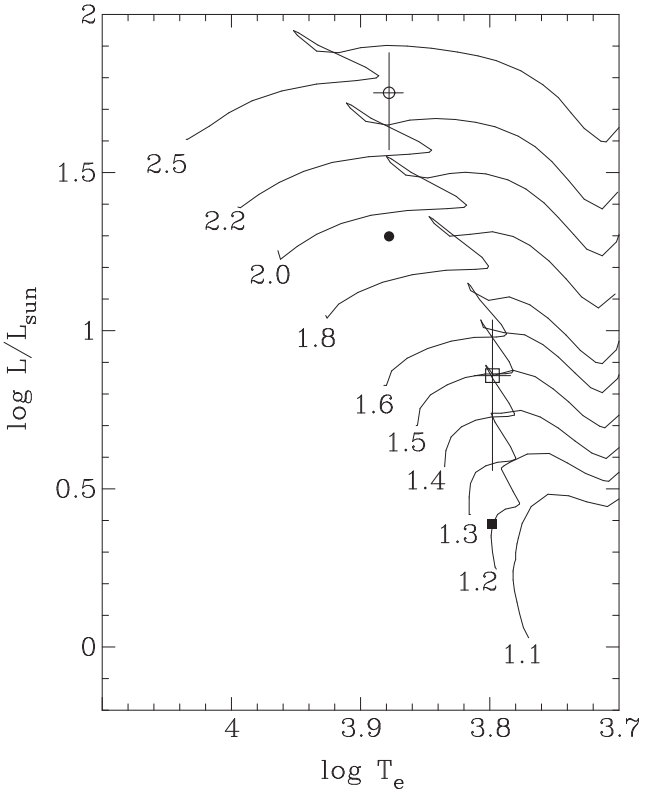

Figure 3. Components Aa and B, having spectral types A8 V and F7: V, respectively, compared with the 1.1–2.5 $M_{\odot}$ solar-composition evolutionary tracks of Girardi et al. (2000). Circle—Aa, square—B. Open symbols are positions computed with a parallax of 0.″00392 ± 0.″00066 (van Leeuwen 2007), solid symbols are positions computed with an adopted parallax of 0.″00667.

parallax of 0.″00296 ± 0.″00077 was smaller than the revised value, corresponding to a larger distance of 338 pc (Perryman & ESA 1997). With that value the resulting stellar properties would be even more discrepant. If the parallax is increased substantially to 0.″00667, corresponding to a distance of 150 pc, the resulting absolute magnitudes for Aa and B become 1.45 and 3.75 mag, respectively, and from the evolutionary tracks (Figure 3) the masses become 1.9 and 1.2 $M_{\odot}$, respectively, which are much more in line with canonical results (Gray 1992). These revised positions result in an age of 1.2 Gyr for component Aa and an age of 2.5 Gyr for component B. This seemingly large difference can be reconciled to a consistent age of 1.2 Gyr for both components if the V magnitude difference is increased by just 0.2 mag, a value that is well within the estimated error for that difference.

From our rotational broadening fits to the Fairborn spectra, we determine $v \sin i$ values of 92 ± 5 km s^{-1} for Aa and 4.5 ± 1.0 km s^{-1} for B. Given the δ Scuti pulsations of Aa, which affect the line profiles, its line widths vary, and so we have increased the estimated uncertainty of the rotational velocity to take this into account. Adopting a rotational inclination of 60°, the same as the orbital inclination suggested below, results in an equatorial rotational velocity of 106 km s^{-1}. The low $v \sin i$ value for component B presumably results from a stellar wind producing magnetic breaking and the fact that this F7: V star is not part of a close binary where tidal forces would spin up its rotation.

Since the significant amplitude of the ellipticity variation (Henry et al. 2004) indicates that the orbital inclination of the short-period system is not low, we adopt an inclination of 60°. Taking the mass of Aa to be 1.9 $M_{\odot}$, combined with the small mass function of only 0.0011 $M_{\odot}$ (Table 2), we find a mass of ~0.2 $M_{\odot}$ for component Ab, corresponding to a mid-M dwarf. Thus, the total estimated mass of Aa plus Ab is 2.1 $M_{\odot}$ and that for component B, the F7 dwarf, is 1.2 $M_{\odot}$. This results in a mass ratio, B/A, of 0.57, which is in excellent agreement with the mass ratio of 0.56 from the long-period orbit. Comparing the minimum masses with the masses from the evolutionary tracks results in an orbital inclination ranging from 49° to 52° for the long-period orbit.

D. Pourbaix (2014, private communication) has found that if one adopts the values of the four long-period spectroscopic elements that are in common with the astrometric elements and solves for the remaining ones, evidence of the long-period orbit is at best marginally present in the *Hipparcos* astrometric data. That orbit produces an inclination of 69° ± 15° and a parallax of just 0.″00231 ± 0.″00077, and the F2 estimator of the goodness-of-fit for this new solution is −0.81. This inclination and parallax appear to be inconsistent with the results found above that require a substantially larger parallax and somewhat lower long-period inclination.

We thank D. Pourbaix, who reexamined the *Hipparcos* astrometric data and provided his results. We also thank D. Barlow, who computed a very preliminary short-period orbit. Astronomy at Tennessee State University is supported by the state of Tennessee through its Centers of Excellence programs.

REFERENCES

Barker, E. S., Evans, D. S., & Laing, J. D. 1967, RGOB, 130, 355
Daniels, W. 1966, Technical Report No. 579, Univ. Maryland, Dept. of Physics and Astronomy
Eaton, J. A., & Williamson, M. H. 2004, Proc. SPIE, 5496, 710
Eaton, J. A., & Williamson, M. H. 2007, PASP, 119, 886
Fekel, F. C. 1999, in ASP Conf. Ser. 185, in Precise Stellar Radial Velocities, IAU Coll. 170, ed. J. B. Hearnshaw, & C. D. Scarfe (San Francisco, CA: ASP), 378
Fekel, F. C., & Griffin, R. F. 2011, Obs, 131, 283
Fekel, F. C., Rajabi, S., Muterspaugh, M. W., & Williamson, M. H. 2013, AJ, 145, 111
Fekel, F. C., Warner, P., & Kaye, A. B. 2003, AJ, 125, 2196
Fitzpatrick, M. J. 1993, in ASP Conf. Ser. 52, Astronomical Data Analysis Software and Systems II, ed. R. J. Hanisch, R. V. J. Brissenden, & J. Barnes (San Francisco: ASP), 472
Flower, P. J. 1996, ApJ, 469, 355
Girardi, L., Bressan, A., Bertelli, G., & Chiosi, C. 2000, A&AS, 141, 371
Gray, D. F. 1992, The Observation and Analysis of Stellar Photospheres (Cambridge: Cambridge Univ. Press)
Handler, G. 1999, MNRAS, 309, L19
Handler, G., & Shobbrook, R. R. 2002, MNRAS, 333, 251
Henry, G. W., Fekel, F. C., & Henry, S. M. 2004, AJ, 127, 1720
Lacy, C. H. S., & Fekel, F. C. 2011, AJ, 142, 185
Lucy, C. B., & Sweeney, M. A. 1971, AJ, 76, 544
Mathias, P., le Contel, J.-M., Chapellier, E., et al. 2004, A&A, 417, 189
Matthews, L. D., & Mathieu, R. D. 1992, in ASP Conf. Ser. 32, Complimentary Approaches to Double and Multiple Star Research, IAU Coll. 135, ed. H. A. McAlister, & W. I. Hartkopf (San Francisco, CA: ASP), 244
Mazeh, T., & Shaham, J. 1979, A&A, 77, 145
Perryman, M. A. C., & ESA 1997, The *Hipparcos* and Tycho Catalogues (Noordwijk: ESA)
Russell, H. N. 1902, ApJ, 15, 252
Scarfe, C. D. 2010, Obs, 130, 214
van Leeuwen, F. 2007, *Hipparcos* The New Reduction of the Raw Data, Vol. 350 (Berlin: Springer)
Wilsing, J. 1893, AN, 134, 89
Wolfe, R. H., Horak, H. G., & Storer, N. W. 1967, in Modern Astrophysics, ed. M. Hack (New York: Gordon and Breach), 251